Supporting information

Sodium Storage Performance of a High Entropy Sulfide Anode with Reduced Volume Expansion

Jianping Ma[1], Jinyi Guo[1], Weizheng Li, Xiaohan Yang, Chengde Huang[*]

Department of Applied Chemistry, School of Chemical Engineering and Technology, Tianjin University, Tianjin, 300072, P.R. China

[*] Corresponding author.
E-mail address: cdhuang@tju.edu.cn (C. Huang)

[1]These authors contributed equally to this work.
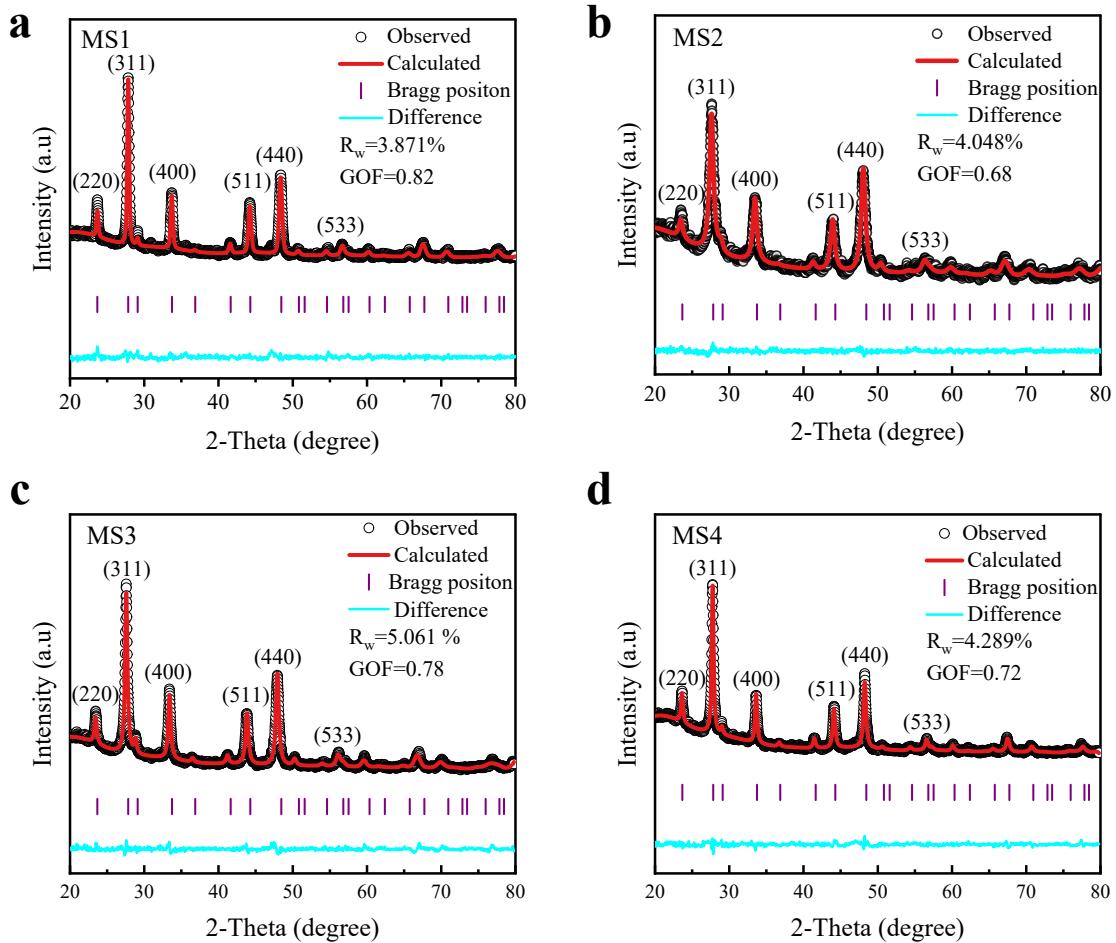
Figure S1 Rietveld refinement of (a–d) MS1–MS4.
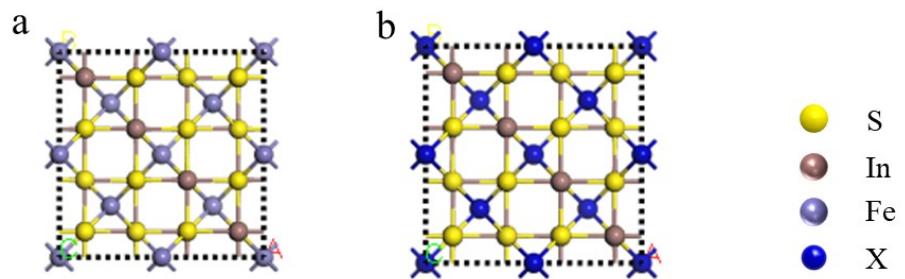
Figure S2 Crystal schematic of (a) MS1 and (b) MS5 material after Rietveld refinement.
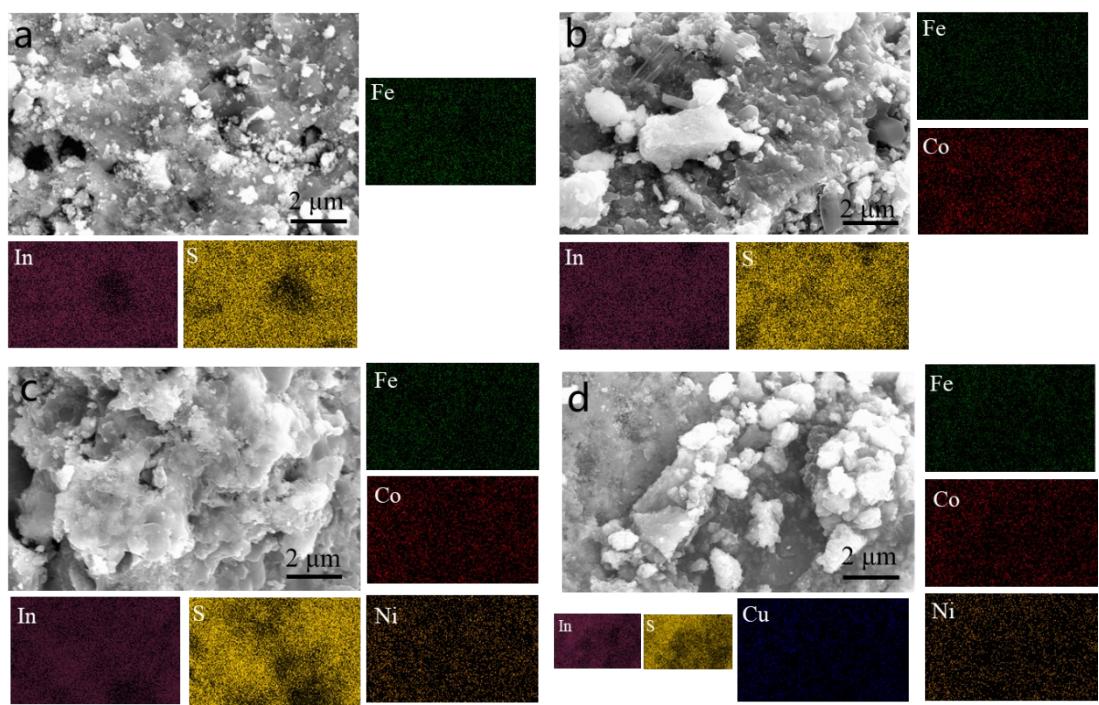
Figure S3 EDS of (a) MS1, (b) MS2, (c) MS3 and (d) MS4.
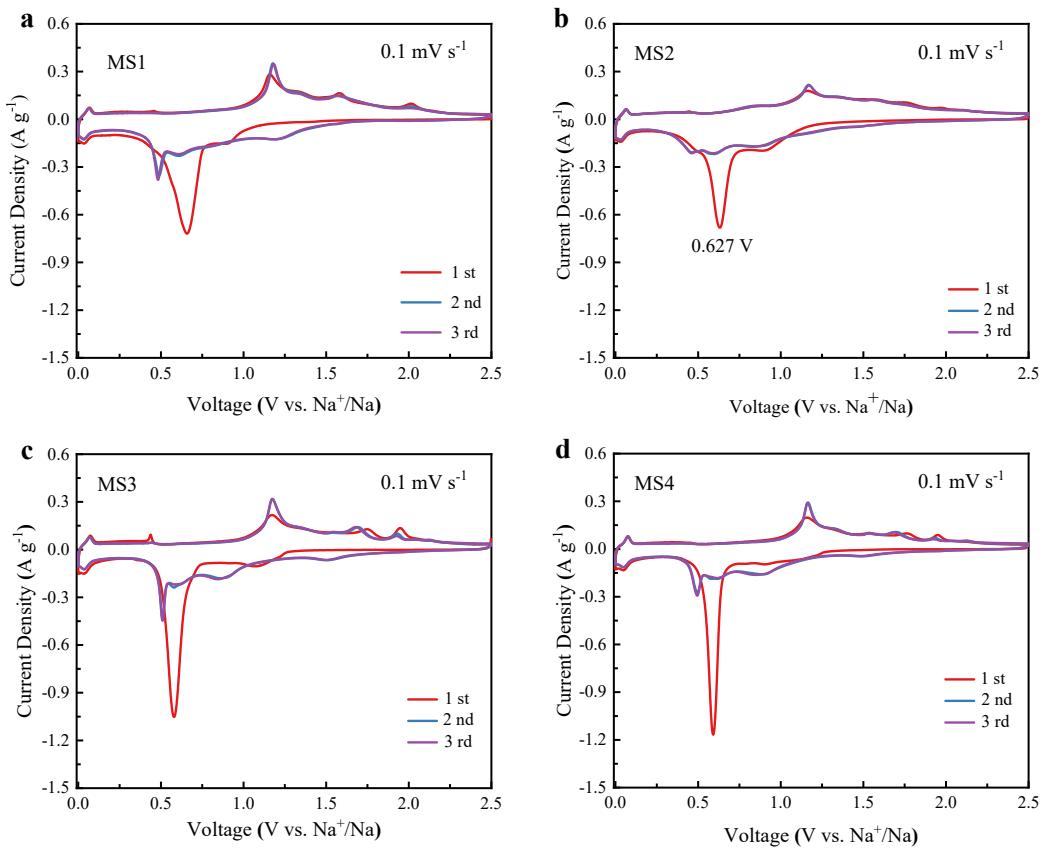
Figure S4 The first three CV curves of (a) MS1, (b) MS2, (c) MS3 and (d) MS4 materials at 0.1 mV s^{-1}.
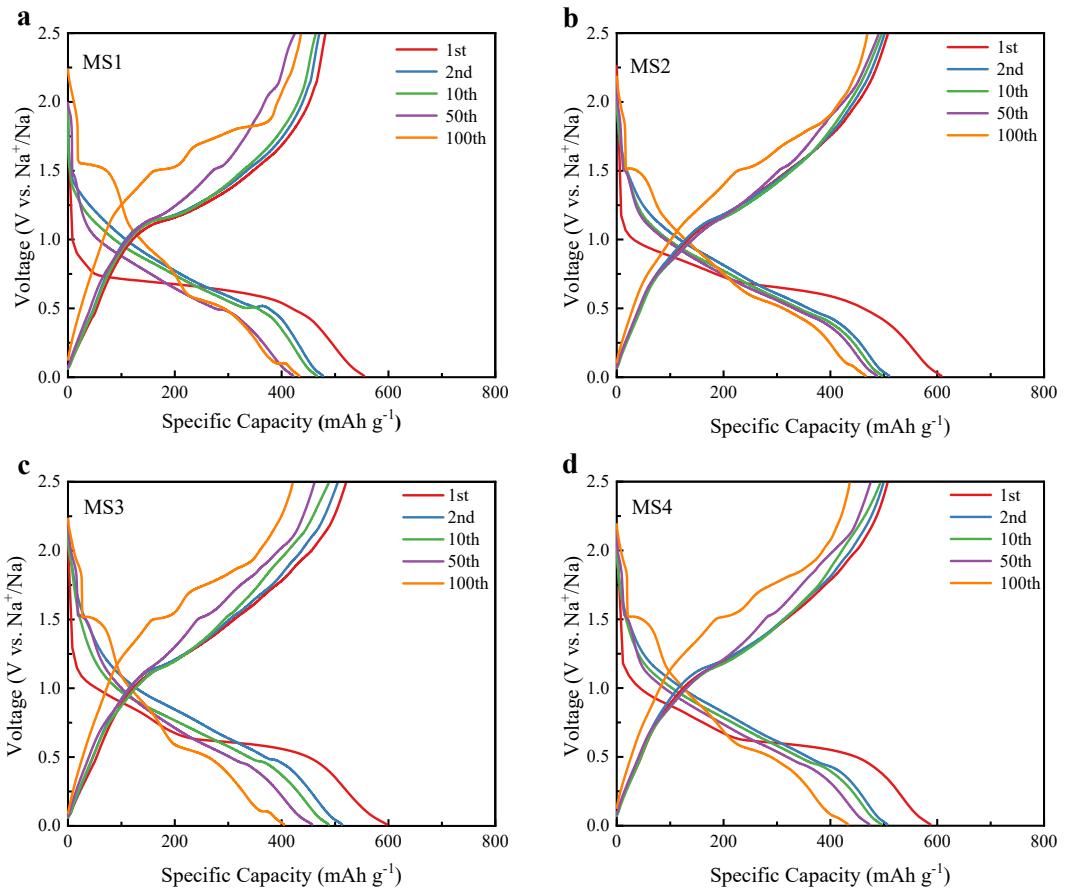
Figure S5 Charge-discharge curves of (a) MS1, (b) MS2, (c) MS3 and (d) MS4 materials at 0.5 A g^{-1}.
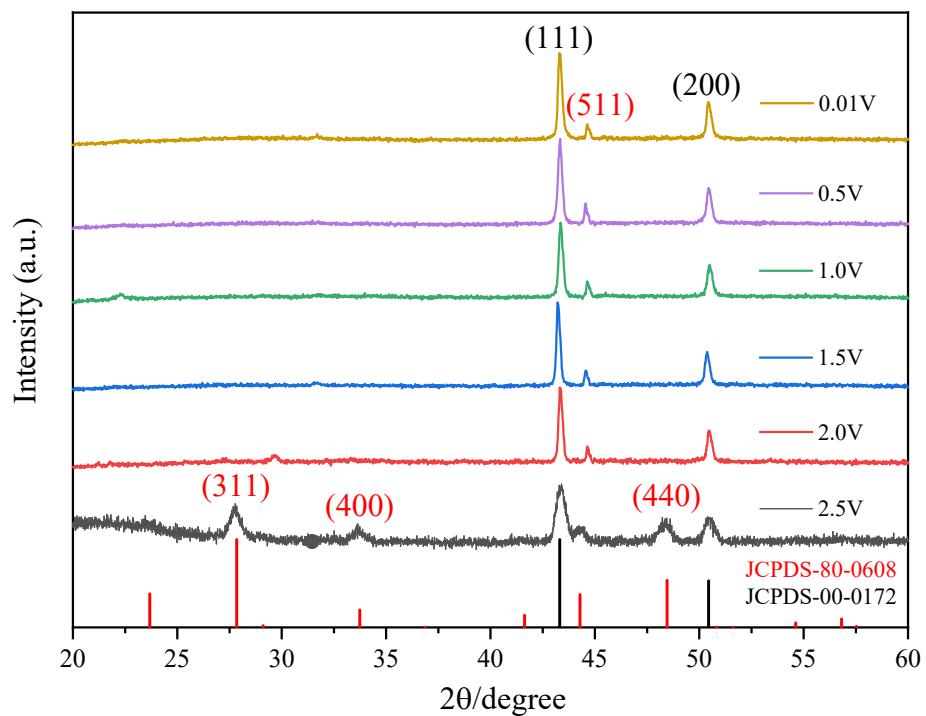
Figure S6 The XRD patterns of the MS5 electrode sheet during the cycling process.
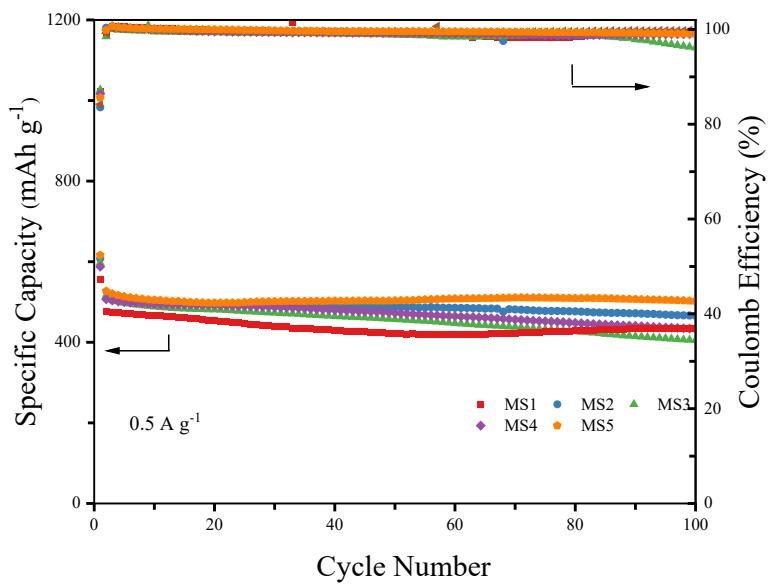
Figure S7 Performance of MS1–MS5 for the first 100 cycles at 0.5 A g⁻¹.

Map
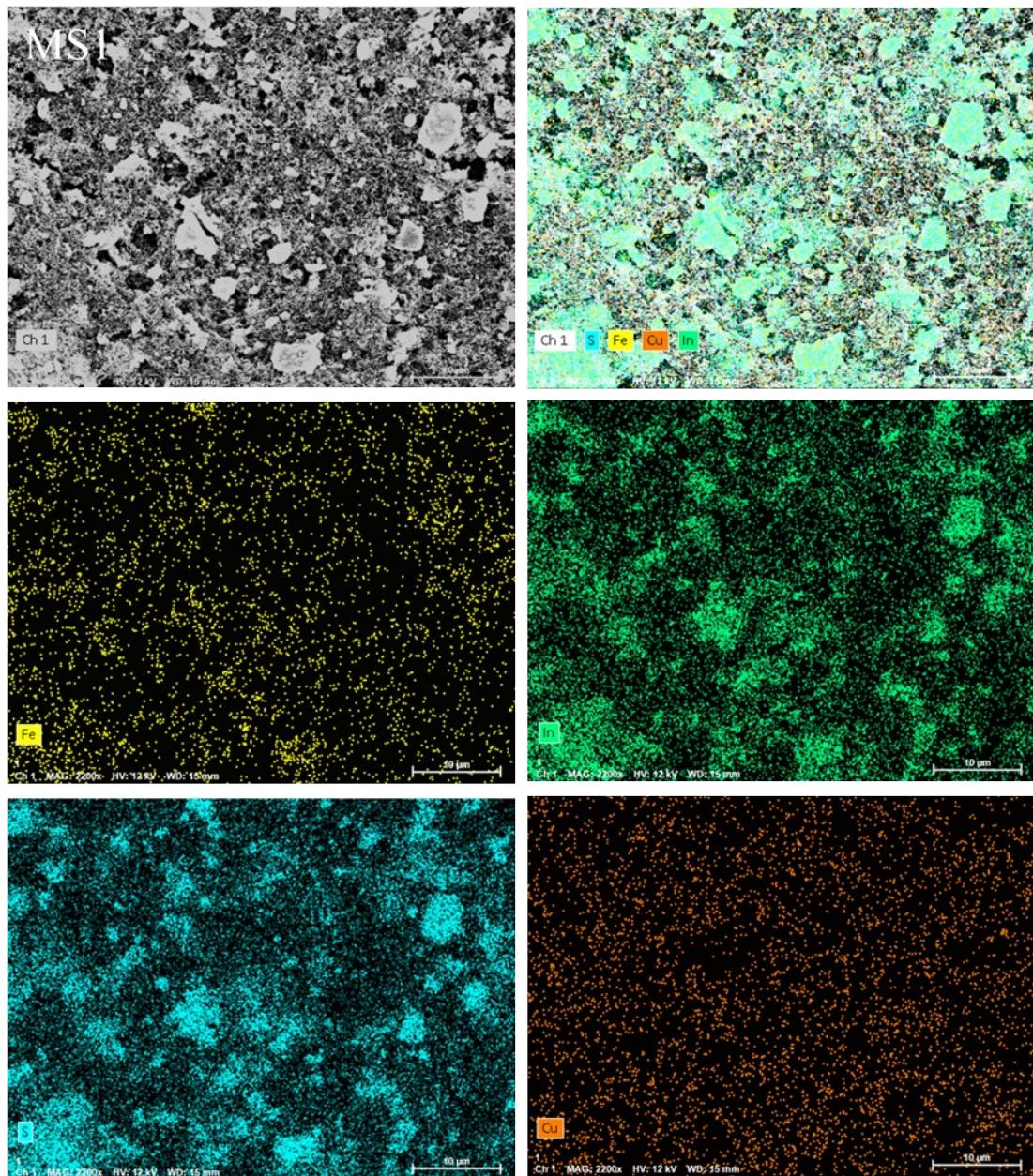
Elements	Fe	In	S	Cu
Normalized mass [%]	12.79	52.41	30.87	3.93
Atom [%]	13.39	26.69	56.30	3.62
Abs. error[mass%] (3σ)	0.86	1.97	1.22	0.36

Figure S8 SEM-EDS images of MS1 before cycling.

Map
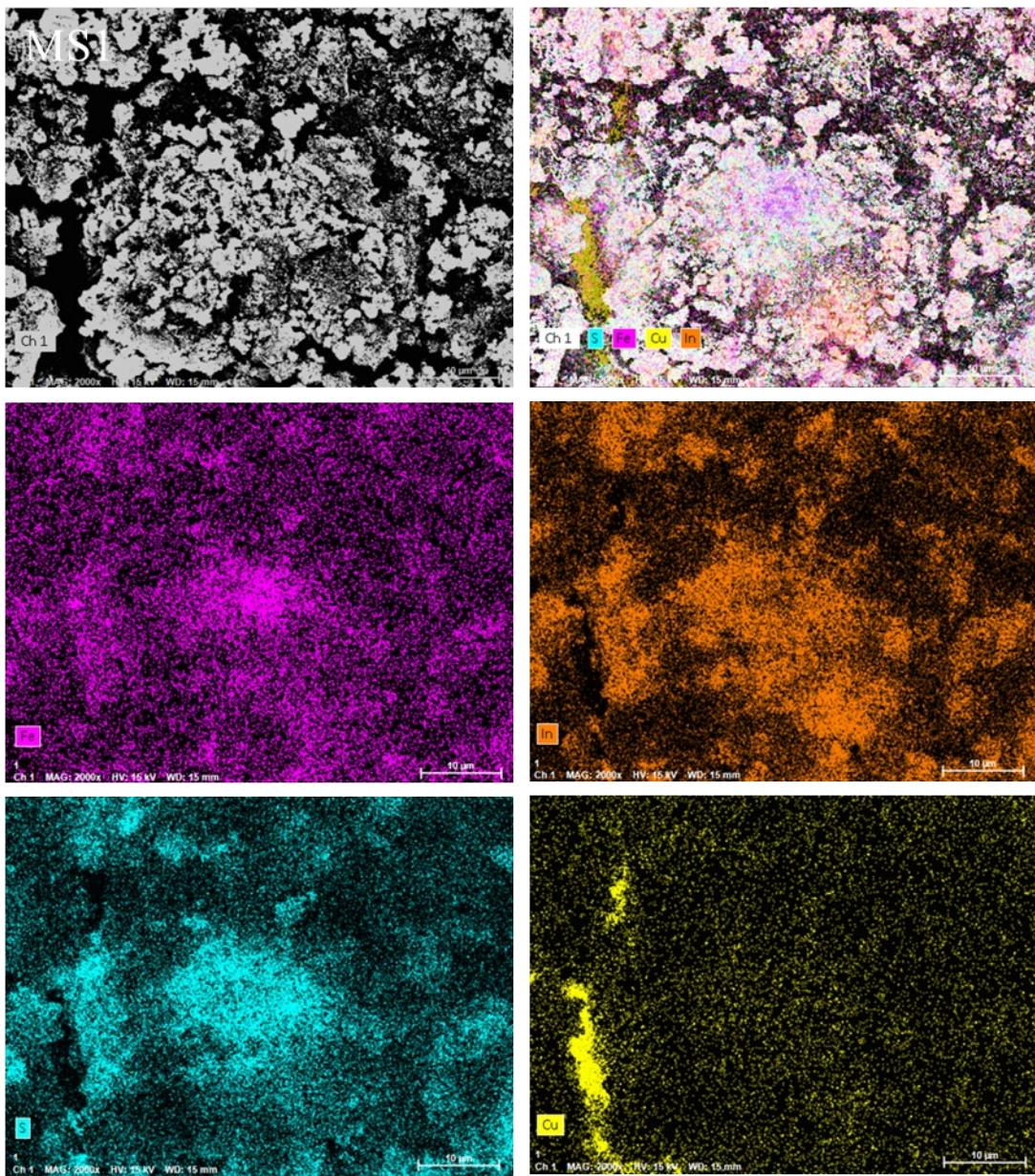
Elements	Fe	In	S	Cu
Normalized mass [%]	13.11	58.35	14.14	14.45
Atom [%]	16.64	35.99	31.26	16.12
Abs. error[mass%] (3σ)	0.41	1.44	0.45	0.57

Figure S9 SEM-EDS images of MS1 after cycling.
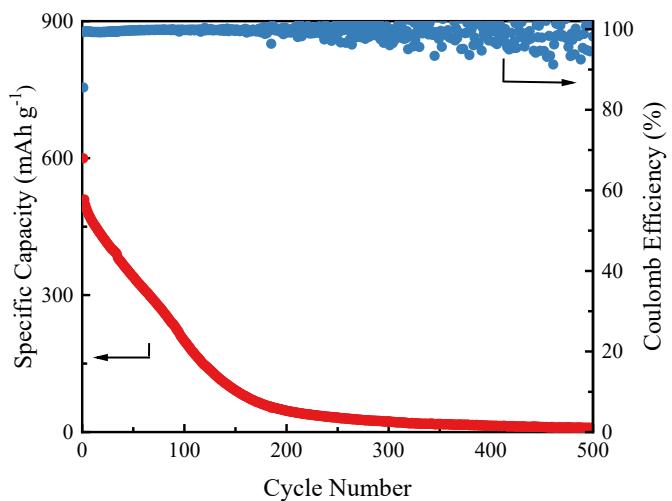
Figure S10 Cycling performance of MS1 at 0.2 A g^{-1} with Al foil as the collector.
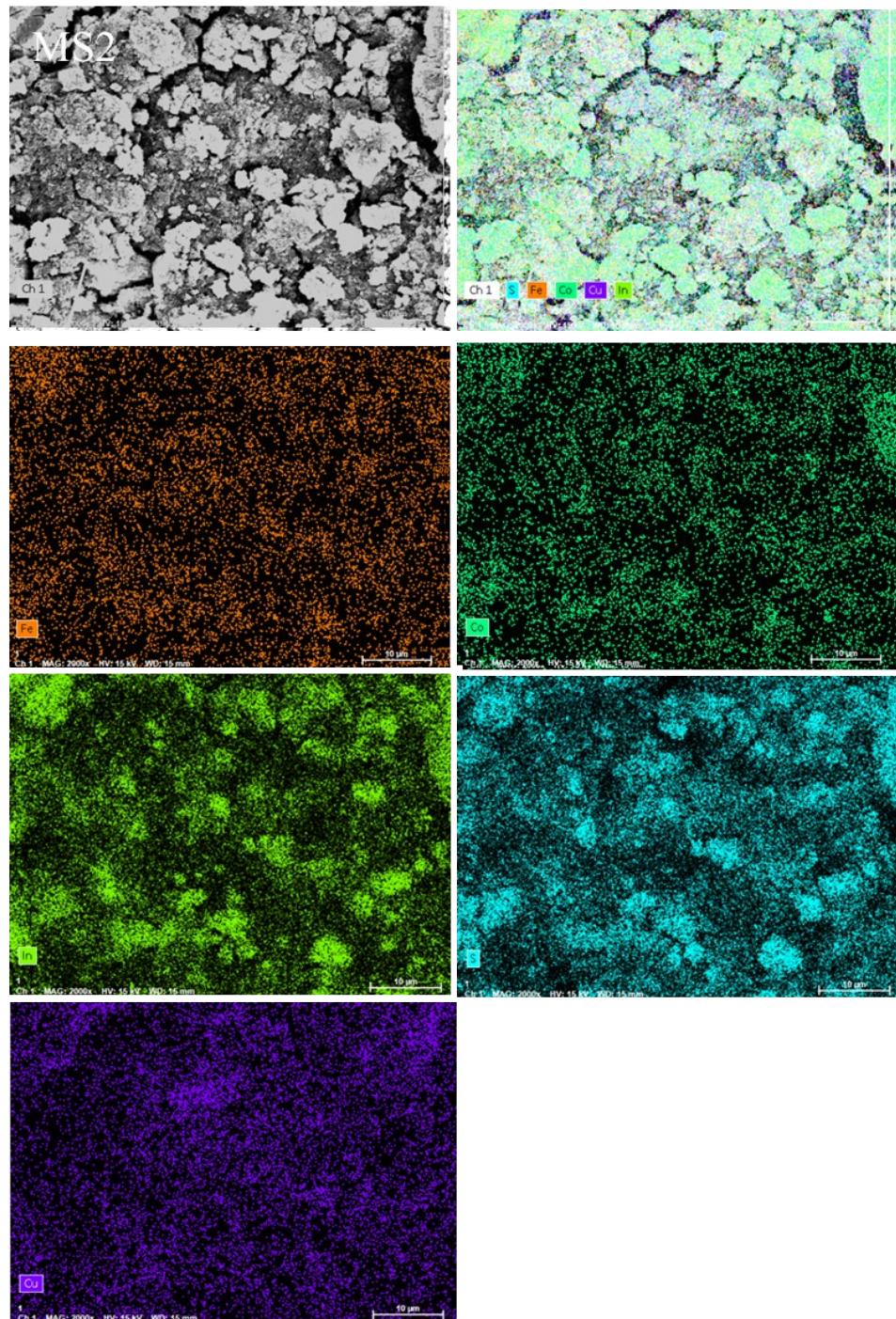
Map

Elements	Fe	Co	In	S	Cu
Normalized mass [%]	4.36	7.01	47.91	18.66	22.06
Atom [%]	5.06	7.71	27.04	37.70	22.49
Abs. error[mass%] (3σ)	0.21	0.31	1.33	0.32	0.91

Figure S11 SEM-EDS images of MS2 after cycling.

Map
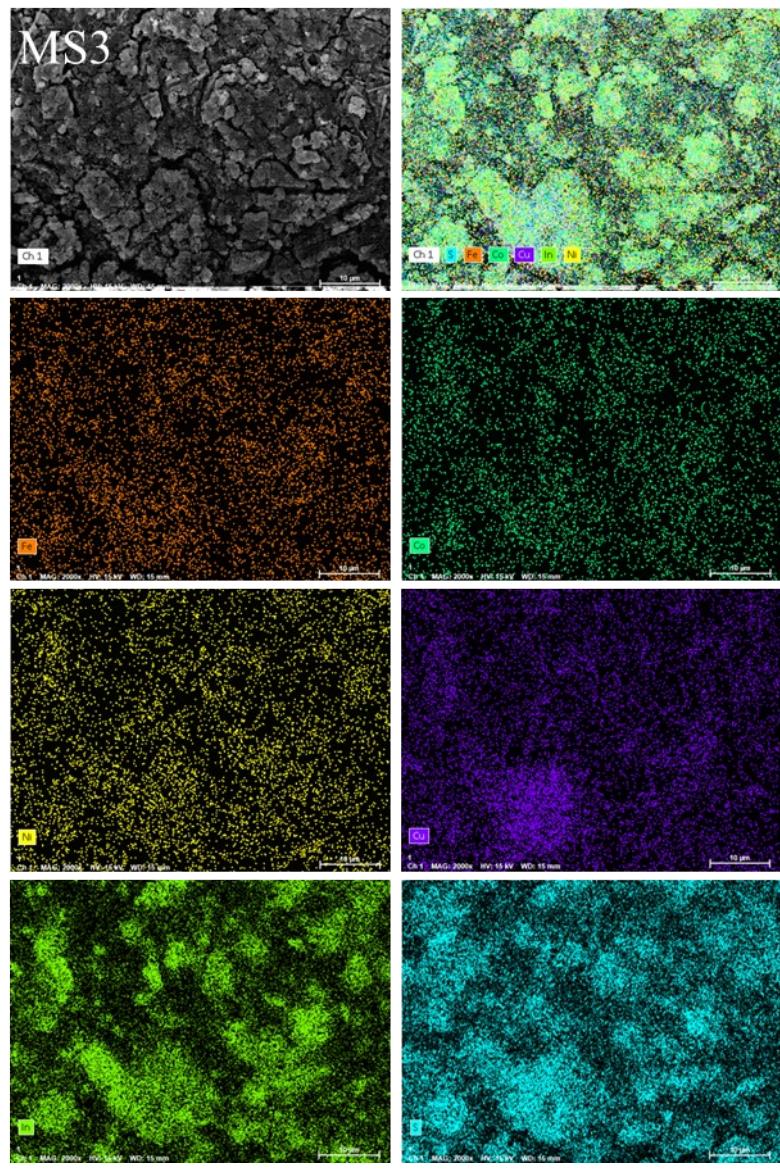
Elements	Fe	Co	Ni	Cu	In	S
Normalized mass [%]	2.49	2.21	2.63	38.78	36.99	16.90
Atom [%]	2.81	2.37	2.82	38.47	20.31	33.22
Abs. error[mass%] (3σ)	0.16	0.18	0.22	1.40	0.87	0.47

Figure S12 SEM-EDS images of MS3 after cycling.
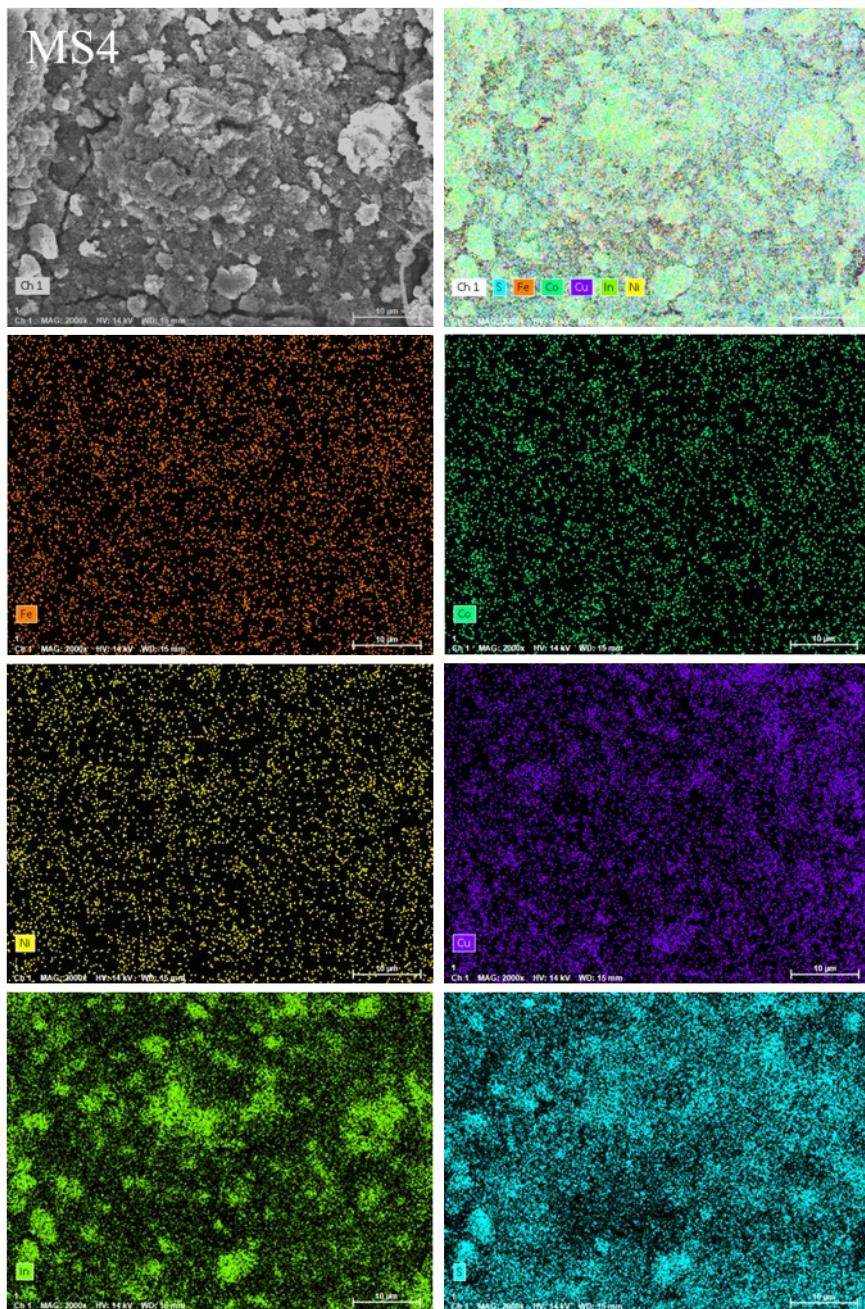
Map

Elements	Fe	Co	Ni	In	S	Cu
Normalized mass [%]	2.81	2.42	6.07	45.28	18.70	24.72
Atom [%]	3.22	2.63	6.63	25.26	37.36	24.91
Abs. error[mass%] (3σ)	0.16	0.18	0.29	1.06	0.53	0.89

Figure S13 SEM-EDS images of MS4 after cycling.

Map
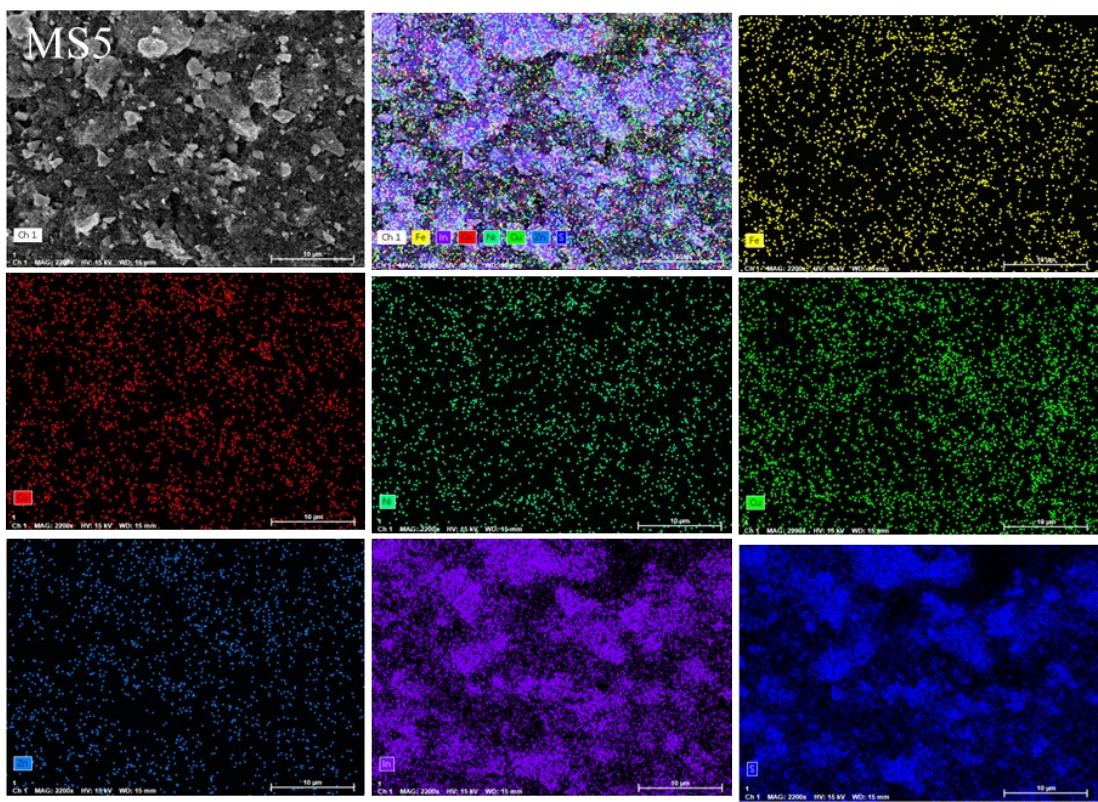
Elements	Fe	Co	Ni	Cu	Zn	In	S
Normalized mass [%]	2.27	2.55	2.25	11.94	2.91	47.46	30.62
Atom [%]	2.36	2.51	2.23	10.91	2.58	23.99	55.43
Abs. error[mass%] (3σ)	0.27	0.33	0.34	0.99	0.53	2.27	1.63

Figure S14 SEM-EDS images of MS5 before cycling.

Map
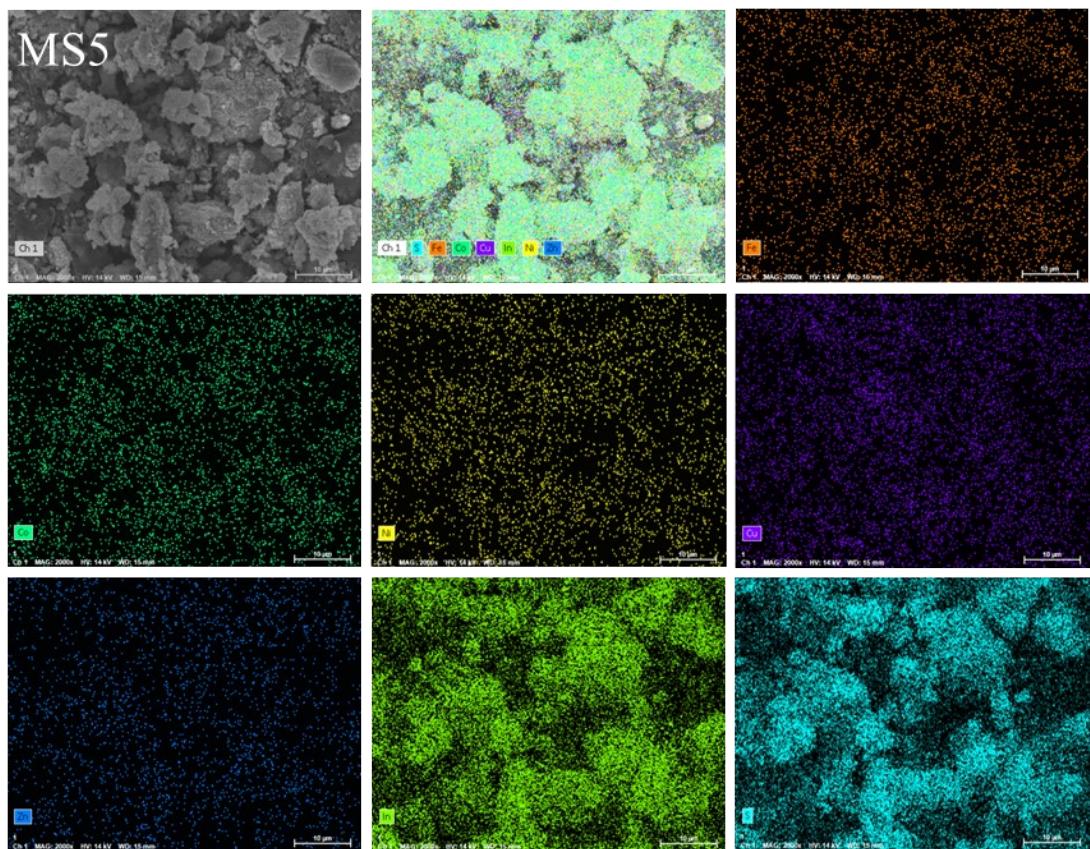
Elements	Fe	Co	Ni	Cu	Zn	In	S
Normalized mass [%]	1.65	3.10	3.18	12.16	2.64	56.77	20.50
Atom [%]	1.97	3.51	3.61	12.74	2.68	32.92	42.56
Abs. error[mass%] (3σ)	0.23	0.34	0.37	0.98	0.52	2.63	1.11

Figure S15 SEM-EDS images of MS5 after cycling.
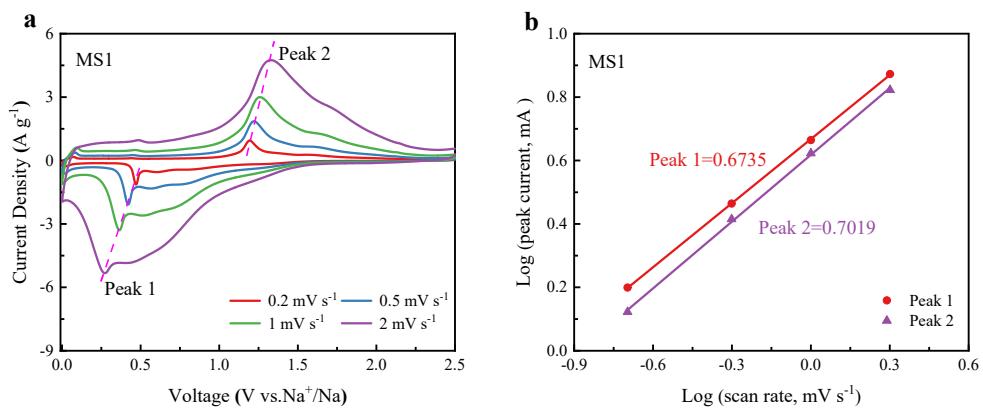
Figure S16 (a) CV curves of MS1 materials at 0.2, 0.5, 1 and 2 mV s^{-1}. (b) linear relationship of MS1 materials between sweep speed and peak current.
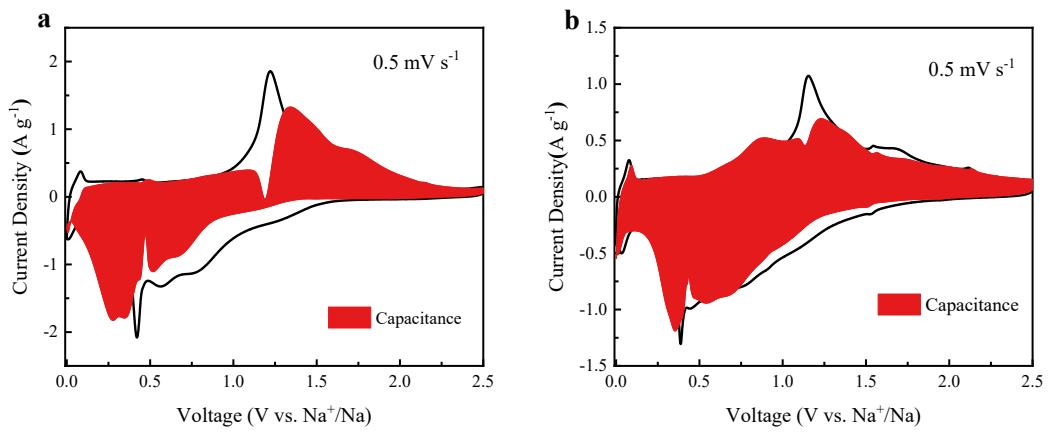
Figure S17 The pseudocapacitance contribution of (a) MS1 and (b) MS5 material at 0.5 mv s^{-1}.
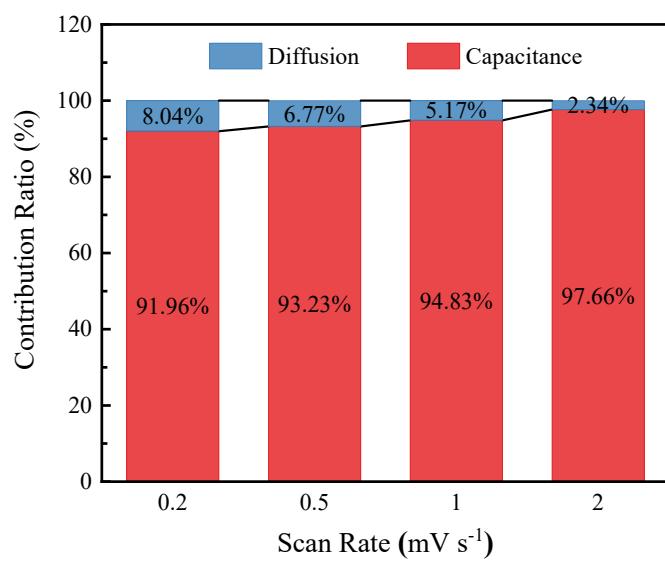
Figure S18 Percentage of pseudocapacitance contribution of MS1 material at different scan rates.
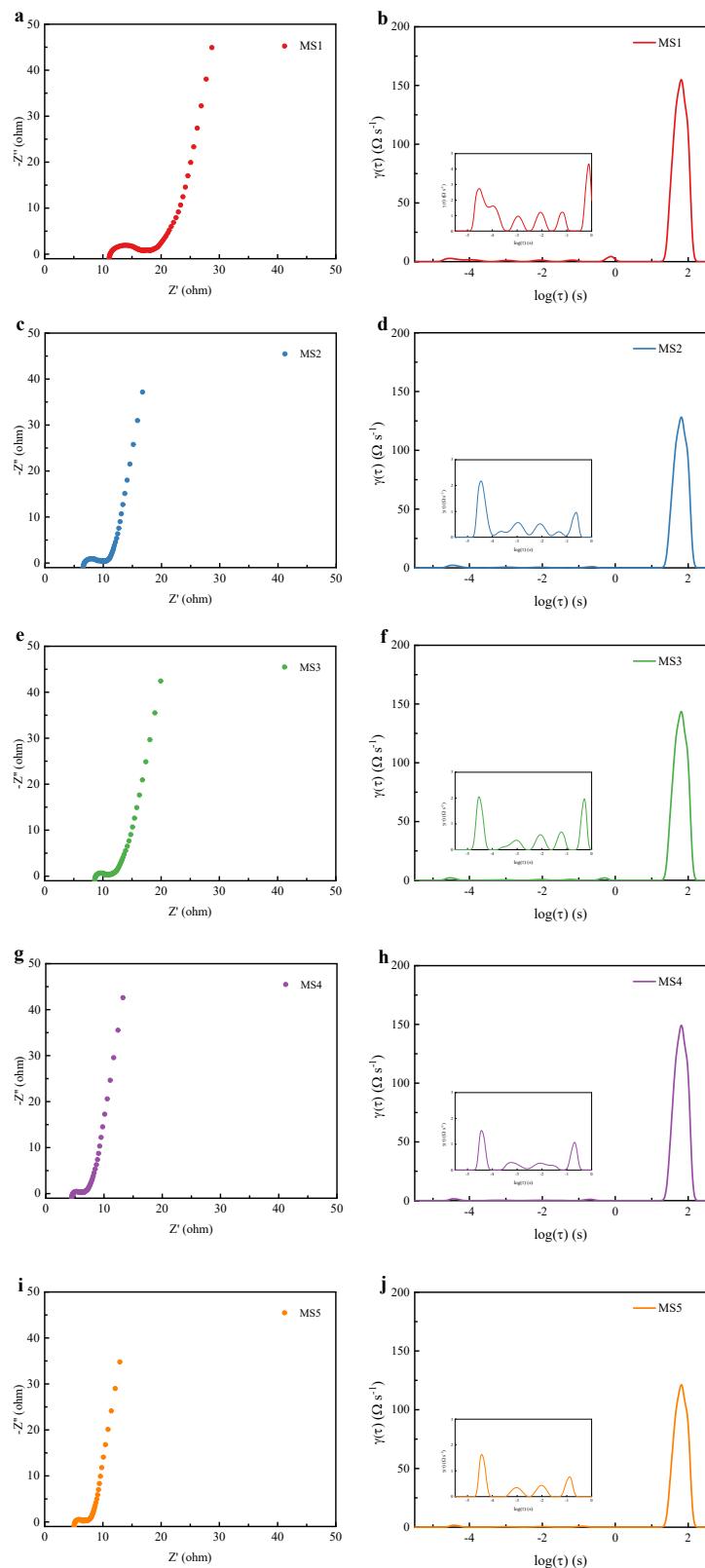
Figure S19 EIS spectra, DRT distributions and localized enlargements of (a, b) MS1, (c, d) MS2, (e, f) MS3, (g, h) MS4 and (i, j) MS5.
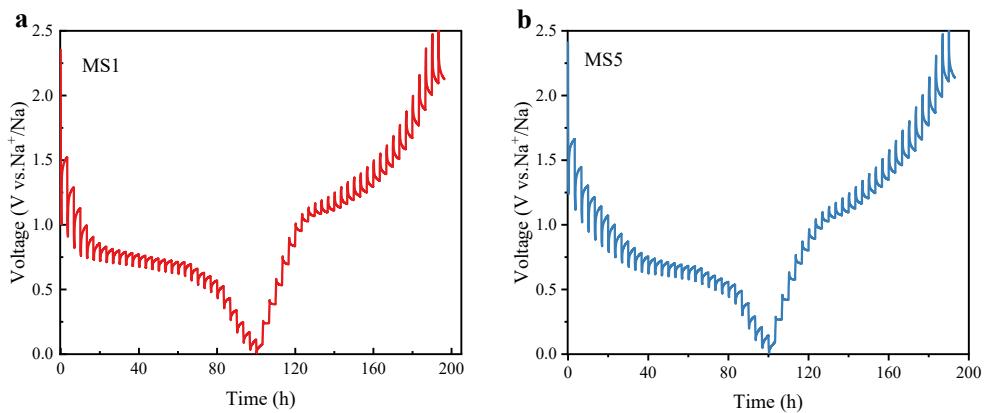
Figure S20 GITT curve of (a) MS1 and (b) MS5 material during the first charge/discharge at 50 mA g^{-1}.
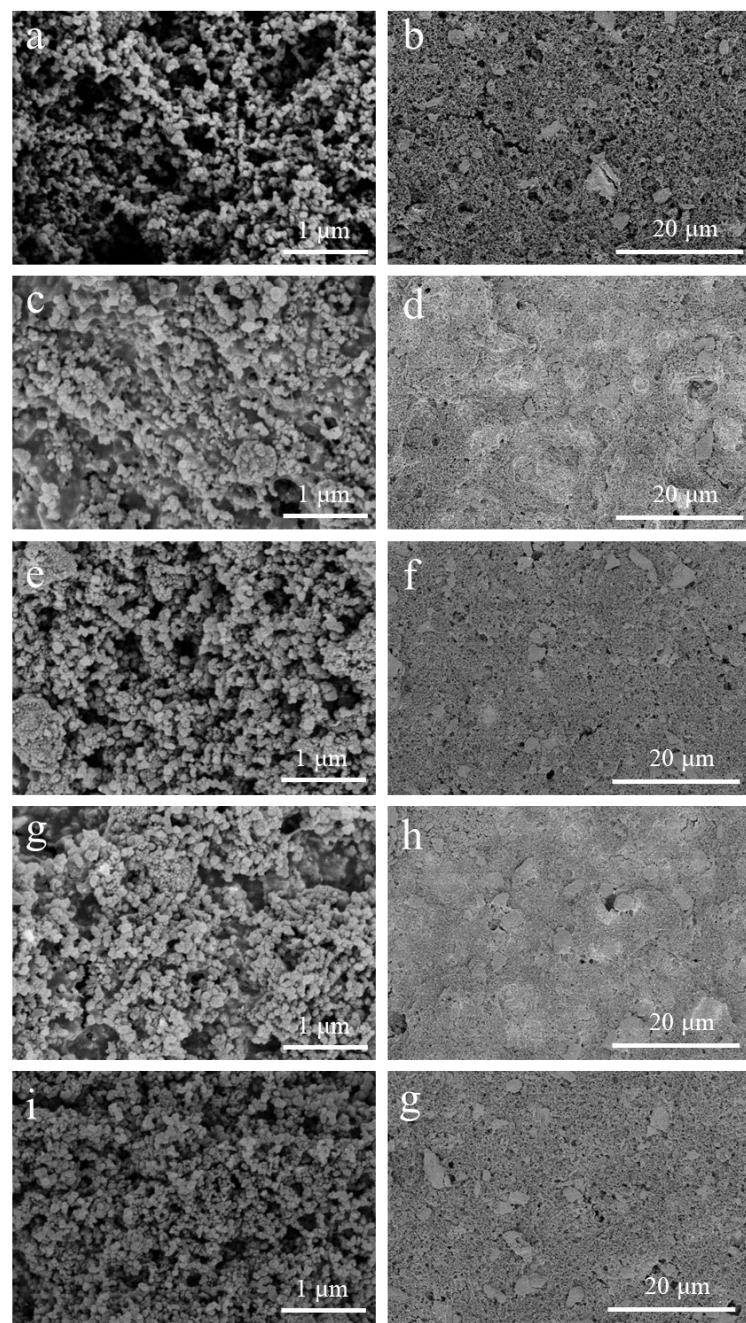
Figure S21 Before cycling (a, b) MS1, (c, d) MS2, (e, f) MS3, (g, h) MS4 and (i, g) MS5 SEM images.
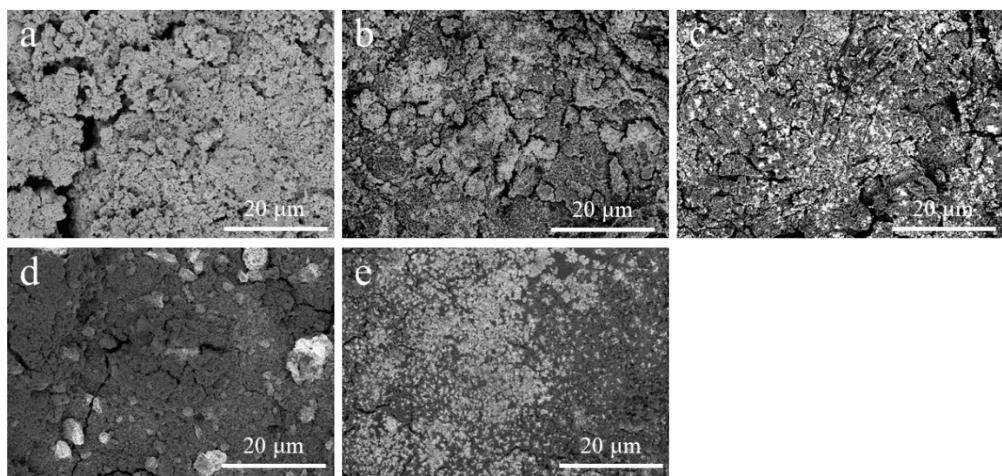
Figure S22 After 100 cycles (a–e) MS1–MS5 SEM images.

S 2p
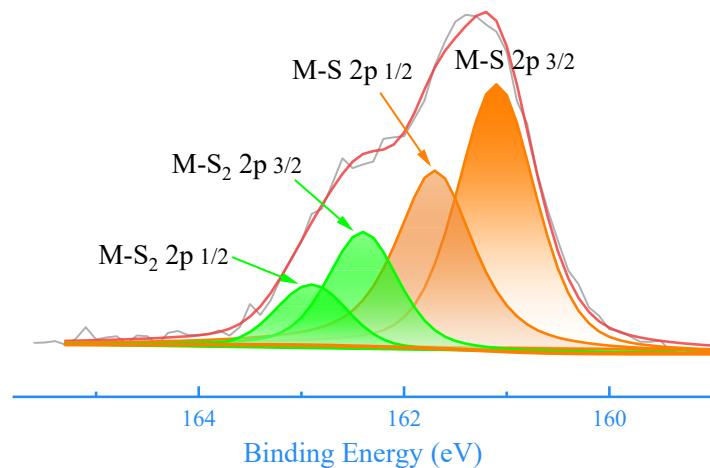
Figure S23 XPS spectra of S 2p for MS1 materials.
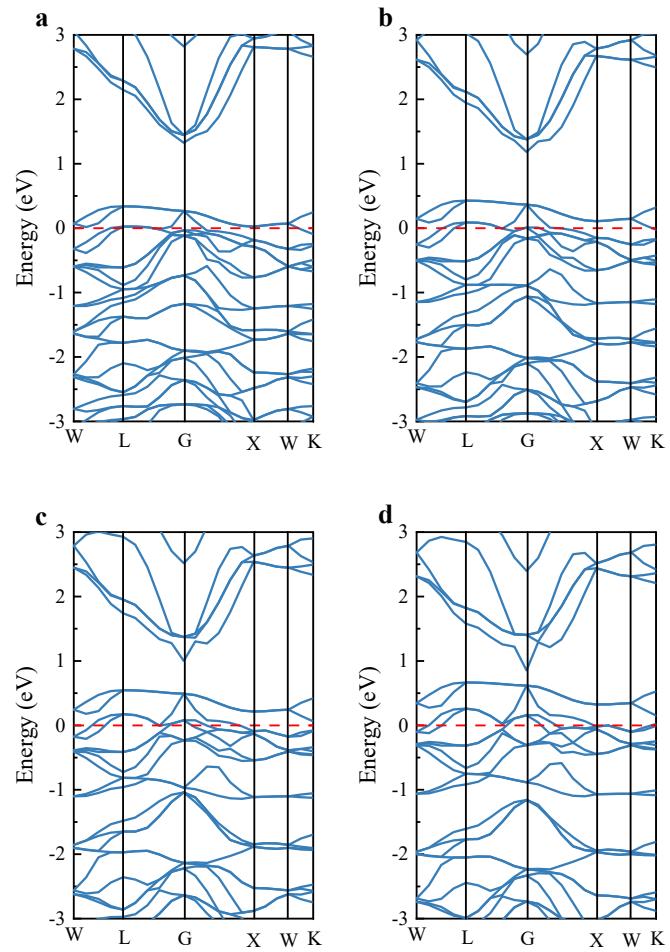
Figure S24 Energy band diagrams of (a) MS1, (b) MS2, (c) MS3 and (d) MS4.
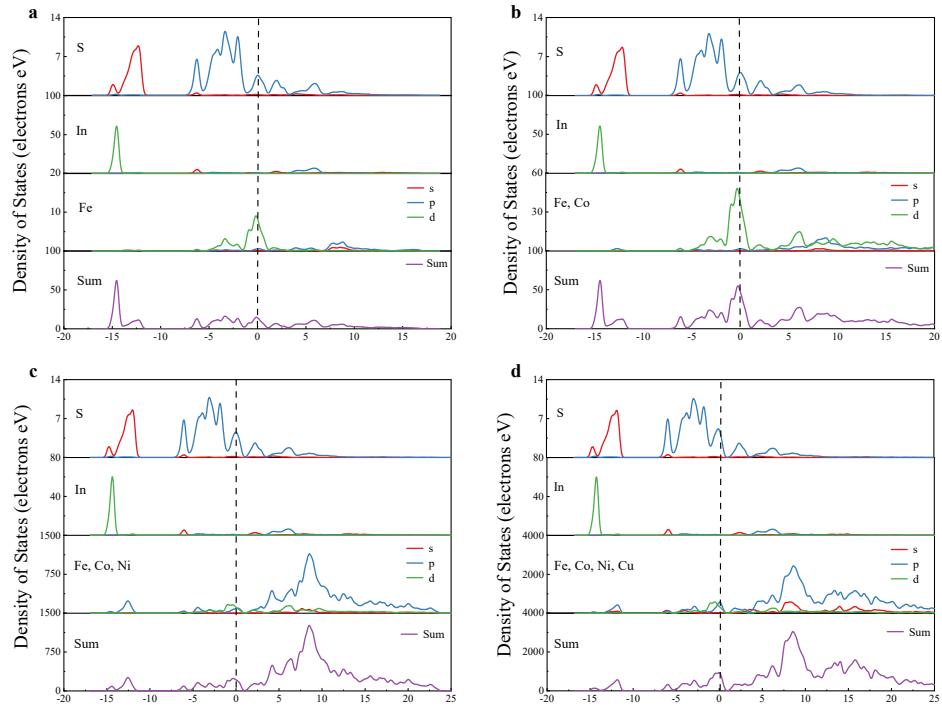
Figure S25 Density of states, fractional density of states diagrams of (a) MS1, (b) MS2, (c) MS3 and (d) MS4.
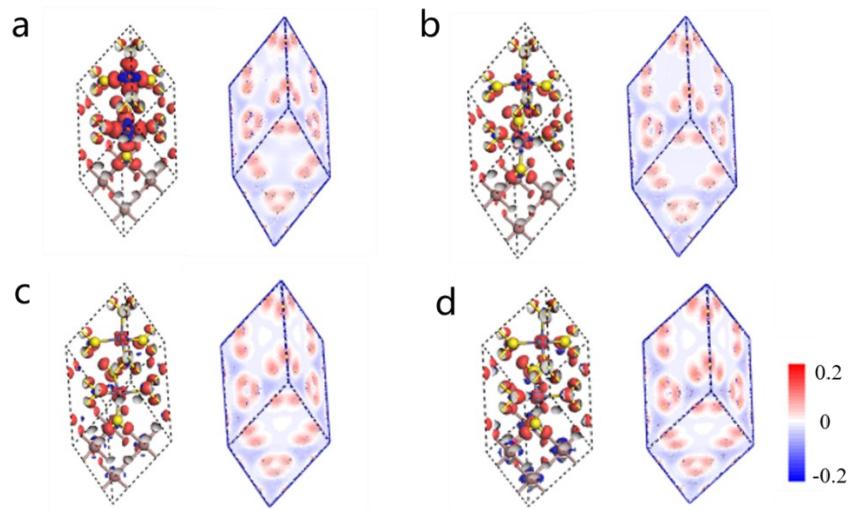
Figure S26 Electron differential charge density plots of (a) MS1, (b) MS2, (c) MS3 and (d) MS4.
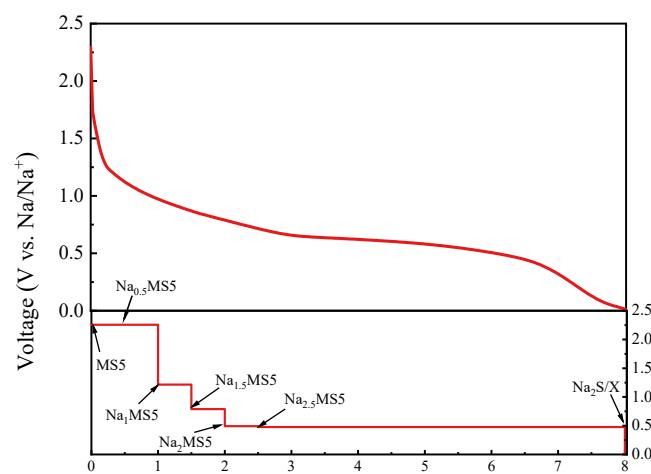
Figure S27 Comparison of the first discharge curve at 0.2 A g^{-1} with theoretical voltage profile from DFT calculation of MS5.
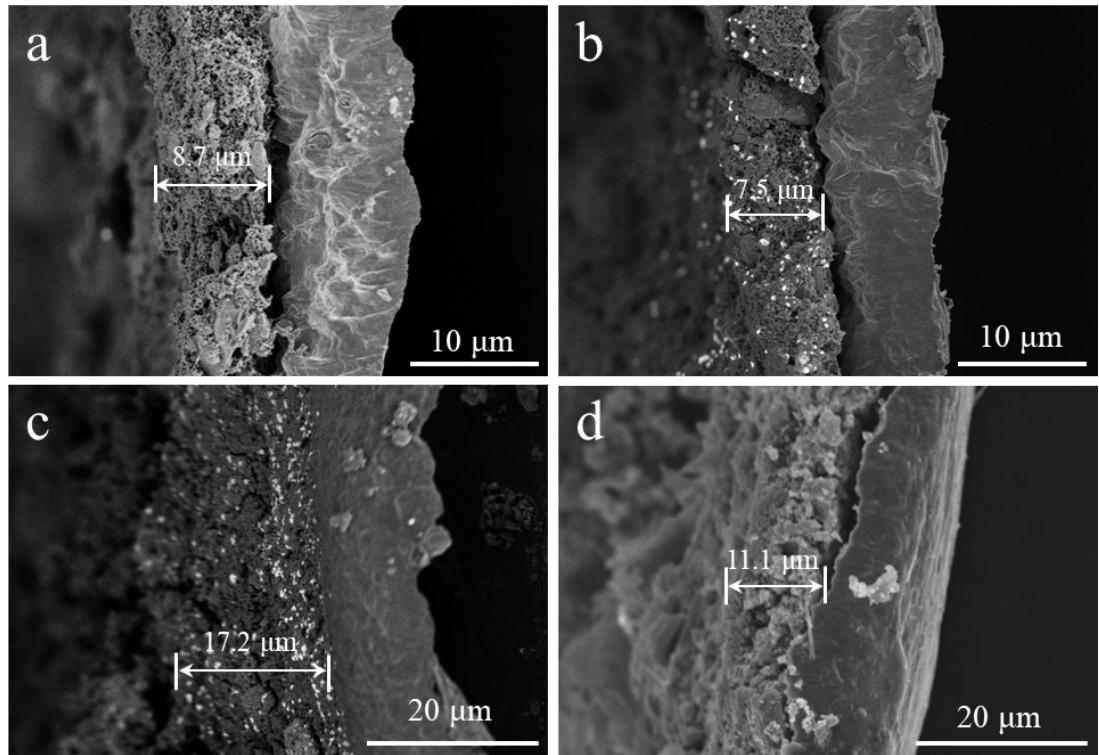
Figure S28 SEM images of the cross-section of the electrode sheets for (a, c) MS1 and (b, d) MS5 before and after cycling.

Table S1 ICP-OES results of element ratios for MS2–MS5

	Fe	Co	Ni	Co	Zn
MS2	0.434	0.566			
MS3	0.300	0.349	0.351		
MS4	0.197	0.264	0.261	0.278	
MS5	0.146	0.205	0.192	0.206	0.252

Table S2 Sodium storage properties of metal sulfides reported in the literature

Metal sulfide anode	Electrolyte	Cycling performance (mAh g^{-1}/A g^{-1}/cycles)	Rate capability (mAh g^{-1}/A g^{-1})	Ref.
CuS@CoS$_2$	1M NaCF$_3$SO$_3$ (DEGDME)	430/0.5/500th	304/5	1
FeS/NiS@NCS	1 M NaClO$_4$ (EC:PC=1:1+5% FEC)	414.6/1/500th	251/5	2
FeSb$_2$S$_4$@Graphite	1M NaPF$_6$ (EC:DMC=1:1+5%FEC)	300/1/100th	186/8	3
V$_2$C/Fe$_7$S$_8$@C	1 M NaClO$_4$ (EC:PC=1:1+5% FEC)	206.2/2/1000th	389.7/5	4
VS$_4$/SnS$_2$@MXene	1 M NaClO$_4$ (EC:DEC=1:1+5% FEC)	187/5/500th	301.5/2	5
L-S-PI@FeS$_2$	1M NaPF$_6$ (DME:CE=1:1)	391/0.2/500th	250/5	6
Cu$_{39}$S$_{28}$-CoS$_2$-ZnS@NC@C	1M NaCF$_3$SO$_3$ (DEGDME)	341.1/5/400th	324.3/	7
NiCoS$_4$@ReS$_2$	1M NaPF$_6$ (EC:DEC=1:1+2.5%FEC)	396/1/500th	297/3	8
Co$_9$S$_8$/CoS@NC	1 M NaClO$_4$ (EC:DEC=1:1+5% FEC)	272.8/1/300th	63.6/6	9
ZnS@MoS$_2$/ NC@rGO	1 M NaClO$_4$ (EC:DEC=1:1+5% FEC)	367/1/200th	308/4	10
(FeCoNiCuZn)In$_2$S$_4$	1 M NaPF$_6$ (DEGDME)	401.8/5/800th	323.4/10	This work

Table S3 R_d, R_{ct} and R_s of MS1−MS5 after DRT analysis

	MS1	MS2	MS3	MS4	MS5
R_d/Ω	75.280	61.183	69.61	70.563	57.454
R_{ct}/Ω	2.223	0.815	1.072	0.599	0.539
R_s/Ω	2.200	1.107	0.811	0.592	0.597

Table S4 Elemental valence changes before and after cycles of MS5

Elements	Valence	Before cycles (%)	After cycles (%)
Fe	2+	88.5	63.43
	3+	11.5	36.57
	0	22.3	49.52
Co	2+	60.3	31.36
	3+	17.4	19.12
	0	17.1	0
Ni	2+	0	50.14
	3+	82.9	49.86
Cu	1+	88.7	100
	2+	11.3	0

Table S5 Formation energies and reaction potentials of MS5 materials upon Na adsorption

Compounds	Formation energy (eV)	Reaction potential (V vs. Na/Na$^+$)
Na$_{0.5}$MS5	-2.256	2.256
Na$_1$MS5	-2.430	1.215
Na$_{1.5}$MS5	-2.368	0.789
Na$_2$MS5	-1.972	0.493
Na$_{2.5}$MS5	-2.388	0.478

References

1. Y. Fang, B. Y. Guan, D. Luan and X. W. Lou, *Angewandte Chemie International Edition*, 2019, **58**, 7739-7743. DOI: https://doi.org/10.1002/anie.201902583
2. Q. Peng, Y. Lu, S. Qi, M. Liang, D. Xu, W. Sun, L.-P. Lv, Y. Wei, S. Chen and Y. Wang, *ACS Applied Energy Materials*, 2022, **5**, 3199-3207. DOI: https://doi.org/10.1021/acsaem.1c03810
3. P. Wang, Y. Ding, Y. Chu, X. Zhu, J. Lin, L. Shao and T. Zeng, *Energy & Fuels*, 2023, **37**, 5577-5585. DOI: https://doi.org/10.1021/acs.energyfuels.3c00106
4. Z. Xiong, H. Shi, W. Zhang, J. Yan, J. Wu, C. Wang, D. Wang, J. Wang, Y. Gu, F.-R. Chen, Y. Yang, B. Xu and X. Yan, *Small*, 2023, **19**, 2206767. DOI: https://doi.org/10.1002/smll.202206767
5. Y.-L. Hou, J.-Z. Chen, B.-H. Zhang, H.-Y. Wang, W.-X. Wen and D.-L. Zhao, *Chemical Engineering Journal*, 2024, **479**, 147914. DOI: https://doi.org/10.1016/j.cej.2023.147914
6. Y. Xie, H. Yang, Y. Huang, Y. Ma, J. Ye and L. Ouyang, *Journal of Energy Storage*, 2024, **84**, 110887. DOI: https://doi.org/10.1016/j.est.2024.110887
7. X. Li, Y. Xiang, R. Deng, X. Wei, X. Liu, Q. Zheng, D. Lin and Y. Song, *Chemical Engineering Journal*, 2021, **425**, 131501. DOI: https://doi.org/10.1016/j.cej.2021.131501
8. Z. Li, R. Sun, Z. Qin, X. Liu, C. Wang, S. Lu, Y. Zhang and H. Fan, *Materials Chemistry Frontiers*, 2021, **5**, 7540-7547. DOI: http://doi.org/10.1039/D1QM00841B
9. T. Zeng, Q. Chen, Y. Ding, X. Xu, D. Feng and D. Xie, *Journal of Energy Storage*, 2024, **76**, 109849. DOI: https://doi.org/10.1016/j.est.2023.109849
10. X. Luo, J. Shao, P. He, K. Li and W. Zhao, *Applied Surface Science*, 2023, **607**, 154821. DOI: https://doi.org/10.1016/j.apsusc.2022.154821